Lewis acid catalysis of phosphoryl transfer from a copper(II)-NTP complex in a kinase ribozyme

Elisa Biondi[1,2], Raghav R. Poudyal[2], Joshua C. Forgy[2], Andrew W. Sawyer[2], Adam W. R. Maxwell[2] and Donald H. Burke[1,2,*]

[1]Department of Molecular Microbiology and Immunology, Bond Life Sciences Center, University of Missouri School of Medicine, Columbia, MO 65211, USA and [2]Department of Biochemistry, Bond Life Sciences Center, University of Missouri School of Medicine, Columbia, MO 65211, USA

ABSTRACT

The chemical strategies used by ribozymes to enhance reaction rates are revealed in part from their metal ion and pH requirements. We find that kinase ribozyme K28(1-77)C, in contrast with previously characterized kinase ribozymes, requires Cu^{2+} for optimal catalysis of thiophosphoryl transfer from GTPγS. Phosphoryl transfer from GTP is greatly reduced in the absence of Cu^{2+}, indicating a specific catalytic role independent of any potential interactions with the GTPγS thiophosphoryl group. In-line probing and ATPγS competition both argue against direct Cu^{2+} binding by RNA; rather, these data establish that Cu^{2+} enters the active site within a $Cu^{2+} \cdot GTPγS$ or $Cu^{2+} \cdot GTP$ chelation complex, and that $Cu^{2+} \cdot$ nucleobase interactions further enforce Cu^{2+} selectivity and position the metal ion for Lewis acid catalysis. Replacing Mg^{2+} with $[Co(NH_3)_6]^{3+}$ significantly reduced product yield, but not k_{obs}, indicating that the role of inner-sphere Mg^{2+} coordination is structural rather than catalytic. Replacing Mg^{2+} with alkaline earths of increasing ionic radii (Ca^{2+}, Sr^{2+} and Ba^{2+}) gave lower yields and approximately linear rates of product accumulation. Finally, we observe that reaction rates increased with pH in log-linear fashion with an apparent $pKa = 8.0 \pm 0.1$, indicating deprotonation in the rate-limiting step.

INTRODUCTION

Artificial ribozymes have been isolated by *in vitro* selection to catalyse a wide range of chemical reactions, although the chemical strategies used by the great majority of them are poorly understood. Revealing how they mediate these transformations is crucial for assessing the feasibility of an RNA-based metabolism, for evaluating RNA world theories of early evolution, for engineering artificial enzymes and other tools for synthetic biology, and for biomedical applications of ribozymes. Those ribozymes that have been studied in detail use several of the same catalytic strategies as protein enzymes, such as Lewis acid catalysis, proton transfer, precise positioning and desolvation of substrates and allosteric regulation, and a small handful of natural and artificial nucleic acid catalysts exploit the chemical reactivity of bound organic cofactors (1–4). Metal ion cofactors accelerate ribozyme catalysis by polarizing and acidifying inner sphere water, by increasing electrophilicity of phosphates and carbonyls, by stabilizing negative charges that develop on transition states, intermediates and products, by assisting in folding and by other mechanisms [reviewed in (5)]. Although Mg^{2+} is the dominant bioavailable divalent cation, the transition metal ions in the first row of the periodic table provide an array of unique chemical capacities, such as variations in Lewis acidity, charge density, preferred bond lengths and coordination geometries. Some metal ions retain their inner hydration sphere and interact via bound water molecules. For others, one or more waters are replaced by direct contact with the ribozyme or substrate(s). The relative stabilities of inner-sphere complexes involving these ions tend to follow the Irving–Williams series (6): $Mn^{2+} < Fe^{2+} < Co^{2+} < Ni^{2+} < Cu^{2+} > Zn^{2+}$. A different series is observed for the affinities of these same ions in complexes with nucleotide mono-, di- and tri phosphates (7) and phosphate mono-esters (5), for which the affinities follow the order $Mn^{2+} > Fe^{2+} > Co^{2+} \approx Ni^{2+} << Cu^{2+} >> Zn^{2+} < Cd^{2+}$. Interestingly, Fe^{2+} has recently emerged as a potential

prebiotic metal ion, based on its likely high concentrations in aqueous solution on the early Earth and on its positive impact on ribozyme folding and catalysis (8).

Ribozymes have been identified that use most of these ions. For example, the hammerhead (HH) ribozyme is active in low concentrations of Mn^{2+}, Co^{2+}, Ni^{2+}, Zn^{2+} and Cd^{2+} (9–14), and RNaseP functions with Zn^{2+} as the sole divalent cation (15). From *in vitro* selections, RNAs have been isolated that assemble Ni^{2+} or Pt^{2+} into a coordinate-covalent RNA-amino acid complex (16) and that interact with immobilized Ni^{2+} or Zn^{2+} on affinity matrices (16,17). Use of divalent copper is highly unusual among structured nucleic acids—in particular among structured RNA—although a few examples have been noted among catalytic DNAs. A DNAzyme has been described that inserts Cu^{2+} and other transition metal ions into a mesoporphyrin ring (18,19), and DNAzymes have been identified that have strict dependence on Cu^{2+} for their catalysis of DNA ligation (20), DNA cleavage (21,22) and DNA-capping activities (23). Several 5′-self-phosphorylating DNAzymes have been shown to use Cu^{2+} either as one among many functional cations [Dk5, (24)] or as a strict requirement [Cu1, Cu4 and Cu7 (25)]. Divalent ions are not always required, however, and the hairpin (HP), HH and Varkud Satellite (VS) ribozymes remain functional in the absence of divalent metals at high concentrations of monovalent ions, relying exclusively on nucleotide functional groups for catalytic chemistry (26–30).

Proton transfer is integral to the mechanisms of ribozymes such as the hepatitis delta virus (HDV), HP, HH, *glm*S, VS and others (31–37). In the HDV ribozyme, for example, a bound metal ion hydroxide is in position to abstract a proton from the 2′OH nucleophile. The active site cytosine C75 is 'histidine-like', in that its apparent pKa is perturbed approximately three pH units from its normal value of 4.2 to neutrality (32), and its N3 is in position to stabilize the leaving group by donating a proton to the ribose 5′OH of G1 (32–34). For self-cleavage by the HP ribozyme, the apparent pKa is ∼6.0, and the deprotonated state of residue A38 has been shown to be important in catalysis (27,38,39). Intriguingly, in molecular dynamics simulations, the N1 of A38 moves into close proximity of the active site 2′OH, where it would be in position to act as general base (40). For tertiary-stabilized HH ribozymes, X-ray crystallography show both G8 and G12 near the scissile bond, with G12 in position to act as general base (36,41), consistent with earlier predictions based on pH rate profiles for site-specifically substituted ribozymes (35,42). The potential role of G12 as general base is further supported by labelling of its N1 via nucleophilic attack on 2′-bromoacetamide (43). Nucleobase-metal ion interactions also appear to contribute to shifting nucleobase pKa values within the active sites of some extended HH ribozymes (9,44), and a suitably positioned Mn^{2+} ion has been observed in HH ribozyme crystals (45). For the *glm*S ribozyme, an active-site guanine is in position to extract a proton from the 2′OH nucleophile (46–48), although it appears from studies of pH dependence of the reaction to participate in catalysis in its neutral, protonated state (49), perhaps by donating a

hydrogen bond to the developing transition state. These observations for natural ribozymes contrast with studies of two previously studied kinase ribozymes (Kin.46 and 2PT3.2 min) (50,51) and by a kinase DNAzyme (Dk1) (25). For all three catalysts, (thio)phosphoryl transfer rates were shown to be independent of pH over the range pH 6.0–8.0 (Dk1 lost activity above 8.0).

The present work details the metal ion and pH requirements for phosphoryl transfer by ribozyme K28(1-77)C. This 58 nt RNA is a variant of ribozyme K28, which was originally selected as a 126 nt species for thiophosphoryl transfer activity using GTPγS as donor (52). Ribozyme K28(1-77)C folds into a compact pseudoknot and transfers a phosphoryl group from GTP (or a thiophosphoryl group from GTPγS) onto itself at two different sites in the primary sequence (Figure 1A) (53). The original selection and functional analysis of ribozyme K28 and its derivatives were performed in the presence of alkaline earth metal ions (Mg^{2+} and Ca^{2+}), transition metal ions (Mn^{2+} and Cu^{2+}) and monovalent cations (K^+ and Na^+) and was buffered to near neutrality with hydroxyethyl-piperazine ethane sulphonate (HEPES, pH 7.5) (52). In the present work, we sought to determine the contributions of each of these components to RNA-catalyzed phosphoryl transfer. We find that both outer-sphere and inner-sphere interactions with hydrated Mg^{2+} play important structural roles. More surprisingly, K28(1-77)C is also the first kinase ribozyme to be fully dependent on Cu^{2+} for optimal activity, and the first for which the rate exhibits a log-linear pH dependence. Other ribozymes from the selection that gave rise to K28 and its derivative K28(1-77)C did not show this dependence on Cu^{2+}. In-line probing (ILP) and competition studies with adenosine triphosphate (ATP) and ATPγS show no evidence of a direct Cu^{2+}-RNA complex and instead reveal that Cu^{2+} enters into the ribozyme as part of a Cu^{2+}•GTP chelation complex, with additional stabilization likely to come from interactions with nucleobase nitrogens in the RNA. The proposed binding mode explains the Cu^{2+} dependence and positions the bound Cu^{2+} to participate in the catalytic step of the reaction by serving as a Lewis acid catalyst.

MATERIALS AND METHODS

Materials

Oligodeoxynucleotides were purchased from Integrated DNA Technologies (Coralville, IA). RNA was transcribed in vitro using phage T7 RNA polymerase, which was overproduced in bacteria and purified in the laboratory. GTPγS and ATPγS were purchased from Sigma (St. Louis). Radiolabelled nucleotides for labelling internal phosphates or internal 2′OH positions ([α^{32}P]-CTP and [γ^{32}P]-GTP, respectively) were purchased from Perkin-Elmer (Waltham, MA). N-acryloyl-aminophenylmercuric (APM) chloride was prepared as described (53–55).

Self-thiokinase reactions

Ribozyme kinetic analyses were carried out essentially as described (53), in most cases using tri-layer
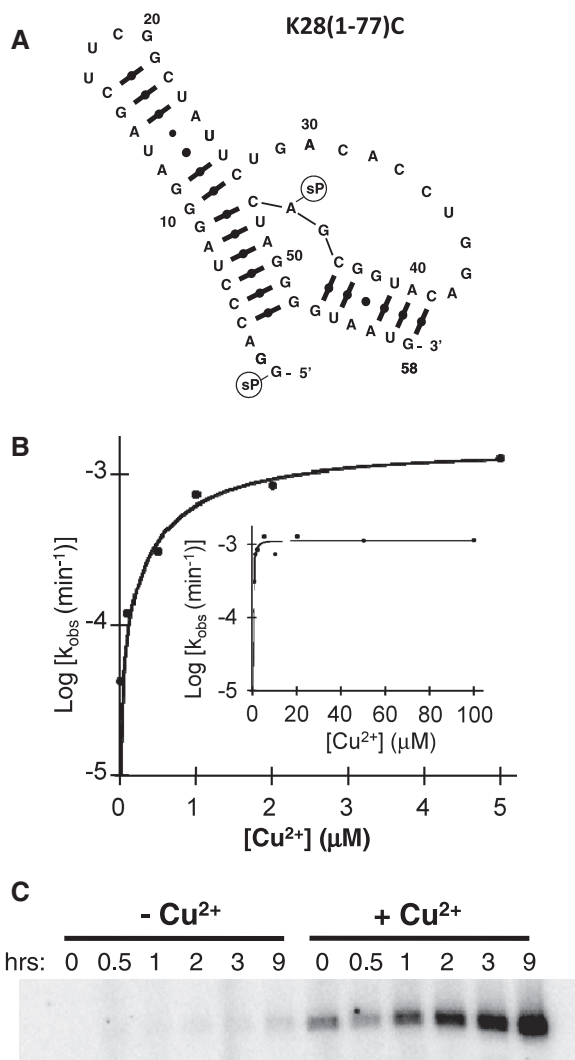
Figure 1. Cu^{2+} dependence of SP. (**A**) Secondary structure of K28(1-77)C. Circled sP indicate the two self(thio)phosphorylation sites; nucleotide G1 represents the major site (52). (**B**) Thiophosphoryl transfer from GTPγS was monitored while titrating Cu^{2+} from 0.01 to 2 μM (0, 0.01, 0.1, 0.5, 1, 2, 5, 10, 50, 100 μM; full data set to 100 μM is shown in inset.) The 'zero-Cu^{2+}' data point was omitted from the plot to allow the log plot. Maximal rate at saturation was $0.00151 \pm 0.00019 \, min^{-1}$. Fitting the initial rates to the quadratic form of a standard 2-state binding equation for a 1:1 complex yielded an apparent dissociation constant for Cu^{2+} ($Kd^{Cu^{2+}}$) of $0.9 \pm 0.4 \, μM$. (**C**) SP reactions (no sulphur) were performed with $[\gamma\text{-}^{32}P]$GTP as phosphoryl donor in SP buffer in the absence or presence of 10 μM Cu^{2+}. Reaction times in hours are given above the lanes.

organomercurial gels to analyse product formation by internally radiolabelled transcripts (52,53,56). In brief, internally radiolabelled K28(1-77)C RNA and other RNA molecules were gel purified, unfolded in water at 85°C for 5 min, then refolded on ice for 5 min by addition of the same 5× self-phosphorylation (SP) buffer used originally to select this ribozyme *in vitro* (52) (1× SP buffer = 6 mM $MgCl_2$, 0.2 mM $CaCl_2$, 0.5 mM $MnCl_2$, 10 μM $CuCl_2$, 200 mM KCl, 15 mM NaCl, 25 mM HEPES, pH 7.5) or modifications of this buffer as detailed in the text. Kinase reactions used 1 μM RNA (50 000–200 000 cpm) and were initiated by adding GTPγS to a final concentration of

0.5 to 1 mM and moving the reaction mixtures to 32°C. Except where noted, reactions were quenched at various times in stop buffer (95% formamide, 15 mM ethylenediaminetetraacetic acid and trace amounts of xylene cyanol and bromophenol blue as tracking dyes). 'Zero' time points were collected immediately after all components were present in the reaction mix. Products were separated on 8% denaturing tri-layered organomercurial gels in which the middle layer contained 100 μg/mL APM [(N-acryloylamino)phenyl]mercuric chloride (52,53,56). Autoradiographs were obtained with a FLA-5000 phosphorimager (FujiFilm) and analysed with MultiGauge software. The fraction of the RNA converted to product at a given time [f(t)] was calculated by dividing the intensities of RNA retained at the APM interface into the sum of all bands within a given lane. First-order exponential rate constants (k_{obs}) and extrapolated plateaus values (f_{max}) of most reactions were obtained by fitting the data to a first-order rate equation using KaleidaGraph (Synergy Software): $f(t) = (f_{max})[1 - \exp^{(-kobst)}]$. Data points in figure 5 are the mean values of at least two replicas for concentrations in which activity was detectable. Data points for the extrapolation of k_{obs} in Figures 1 and 5 were the mean values of at least three replicas for concentrations in which activity was detectable and were fit to a linear equation.

Self-^{32}P-kinase reactions for Cu^{2+}/sulphur dependence

Ribozyme K28(1-77)C was transcribed without radiolabel, gel purified, unfolded in water at 85°C for 5 min, then refolded on ice for 5 min by addition of 5× SP buffer or 5× SP buffer lacking Cu^{2+}. Kinase reactions used 1 μM RNA and were initiated by adding $[\gamma\text{-}^{32}P]$GTP to a final concentration of 0.6 μM and moving the reactions mixtures to 32°C. After the indicated times (0, 0.5, 1, 2, 3, and 9 h), samples were moved to ice and ethanol precipitated immediately by addition of NaOAc, glycogen and ethanol to remove excess non-incorporated radiolabelled GTP. After resuspension in 1× gel loading buffer, samples were analysed on 8%, 8 M urea denaturing polyacrylamide gels as aforementioned.

Self-thiokinase reactions with competitors

K28(1-77)C was unfolded and refolded as aforementioned. ATP or ATPγS was added to a final concentration of 2 mM and kept in ice for 5 min. Donor GTPγS was added to final concentration of 0.5 mM, followed where indicated by addition of supplemental Cu^{2+} to a final concentration of 30 μM.

ILP analysis

Ribozyme K28(1-77)C was 5′-end labelled using $[\gamma\text{-}^{32}P]$ATP, unfolded at 85°C for 5 min, and then refolded by addition of SP buffer with or without $CuCl_2$, and modified to contain 25 mM TRIS (2-Amino-2-hydroxymethyl-propane-1,3-diol) (pH 8.0) in place of 25 mM HEPES (pH 7.5). Competitors, donor and supplemental Cu^{2+} were added in the same order as described earlier in the text. ILP reactions were carried out at room temperature and stopped after 10 h by addition of half

a volume of 95% formamide and 50 mM ethylene-diaminetetraacetic acid. Digestion products were then separated on an 8% denaturing polyacrylamide gel electrophoresis gel, and autoradiographs were analysed as aforementioned.

Self-thiokinase reactions for pH dependence

SP buffer was modified as follows: 25 mM [2-(*N*-morpholino)ethanesulphonic acid] (MES) was used in place of HEPES for pH 5.5, 6.0, 6.5, 6.8; HEPES was used for pH 6.8, 7.0, 7.2, 7.5, 7.8, 8.0; and TRIS was used at pH 8.0, 8.2, 8.5, 8.8, 9.0, 9.5. Owing to precipitation of manganese at elevated pH, this cation was eliminated in all SP buffers used in the pH study. Control reactions performed over the pH range 5.5–8.0 in HEPES verified that activity remains the same with and without Mn^{2+} (data not shown), thereby validating this approach. Very low product accumulation at the lowest pH values (MES buffer) precluded fitting to a first-order exponential rate equation. Rates for these low pH values were obtained from the slope of the line of best fit through these data, adjusted to an assumed plateau of 66% (plateau values for the HEPES and TRIS data are $66 \pm 7\%$ conversion to product). The observed rate constants were then fit to a standard equation for a one-proton transfer: $k_{obs} = k_{max}/[1 + 10^{(pKa-pH)}]$. Kinetic reactions were performed at least in duplicate.

RESULTS

A Cu^{2+}-dependent kinase ribozyme

Ribozyme K28, which is the 126-nt parent form of the 58-nt ribozyme K28(1-77)C, was originally selected for thiophosphoryl transfer activity in SP buffer, which contains monovalent ions (200 mM K^+ and 15 mM Na^+), divalent alkaline earth ions (6 mM Mg^{2+} and 0.2 mM Ca^{2+}) and divalent transition metal ions (0.5 mM Mn^{2+} and 10 μM Cu^{2+}). To begin to understand the contributions of each of these ions to thiophosphoryl transfer activity by ribozyme K28(1-77)C, reactions were carried out in SP buffer in which individual components were omitted. Surprisingly, the ribozyme was essentially inactive without Cu^{2+}. When product formation was monitored, as Cu^{2+} was titrated from 0.01 to 100 μM in the presence of all of the other buffer components, initial rates increased quickly at sub-micromolar concentrations and reached a plateau near the concentration of the RNA (1 μM), with little additional change at still higher concentrations (Figure 1B). Fitting the initial rates to the quadratic form of a standard two-state binding equation yielded a good fit for a 1:1 stoichiometry and an apparent dissociation constant for Cu^{2+} (Kd^{Cu2+}) of 0.9 ± 0.4 μM, which was close to the concentration of RNA used in the assay.

Cu^{2+} is considered to be 'borderline' on the Pearson scale of hard and soft metal ions, and it associates well with 'soft' ligands such as nitrogen and sulphur (57). To determine whether the observed Cu^{2+} requirement is the result of essential interactions between the Cu^{2+} and the thiophosphoryl group of the GTPγS donor,

non-radiolabelled K28(1-77)C RNA was incubated with [γ-^{32}P]GTP in SP buffer with and without Cu^{2+}. Accumulation of radioactivity in the RNA under these conditions indicates sulphur-independent SP by K28(1-77)C. As with the GTPγS donor, product formation from the GTP donor occurred much more vigorously when Cu^{2+} was present, even though there is no sulphur in the GTP donor (Figure 1C). Therefore, the observed requirement for Cu^{2+} in both GTP-dependent and GTPγS-dependent reactions indicates a specific function of the metal ion and not a spurious consequence of having used GTPγS during the initial selection. Therefore, all further reactions included 10 μM Cu^{2+} unless otherwise noted.

Uniqueness of the Cu^{2+} dependence of kinase ribozyme K28

We next sought to determine whether other divalent ions could substitute for Cu^{2+} and whether other ribozymes from the same selection as K28 displayed a similar dependence on Cu^{2+}. Little or no product was observed in overnight reactions when 10 μM Cu^{2+} was replaced with this same concentration of transition metal ions (Cr^{3+}, Co^{2+}, Ni^{2+}, Cd^{2+}, Mn^{2+} and Zn^{2+}) or alkaline earth metals (Mg^{2+}, Ca^{2+}, Sr^{2+} and Ba^{2+}), in the presence of the other buffer components (Figure 2, data not shown). These other metal ions are therefore poor substitutes for 10 μM Cu^{2+}. Because Cu^{2+} binds phosphate more tightly than do these other metal ions (5,58), we next monitored product yields as a function of metal ion concentration. There is a modest increase in product formation when 10 μM Cu^{2+} is replaced with at 100–500 μM Mn^{2+} or Ni^{2+}, but strong inhibition is observed for Zn^{2+}, Co^{2+} and potentially Cd^{2+} at ≥ 100 μM concentrations, perhaps because of non-specific binding to the RNA. Therefore, the role played by Cu^{2+} cannot be fully provided by these other divalent metal ions, which can only support sub-optimal activity (at best) even at 10- to 100-fold higher concentrations.

The *in vitro* selection that gave rise to kinase ribozyme K28 also produced several other ribozymes that could be classified into at least three different families based on their secondary structures (52). Because all of these ribozymes were selected under identical ionic conditions, two ribozymes from each structural family were tested for Cu^{2+} dependence by performing the self-thiphosphorylation reaction in the absence and presence of 10 μM Cu^{2+}. Although ribozymes K28(1-77)C and K28 showed the expected dependence on Cu^{2+}, all six of the other ribozymes produced at least as much product in the Cu^{2+}-depleted SP buffer as they did in the complete SP buffer, and K5 and K6 yielded slightly more product when Cu^{2+} was omitted (Figure 3). Cu^{2+} dependence is therefore not a widespread characteristic among the ribozymes that were selected in the presence of Cu^{2+} and is unique for K28 and its derivatives.

ILP identifies RNA binding by GTP and GTP-Cu^{2+}, but not by Cu^{2+} alone

ILP assays were used to determine whether ribozyme K28(1-77)C uses Cu^{2+} to fold into its active structure.
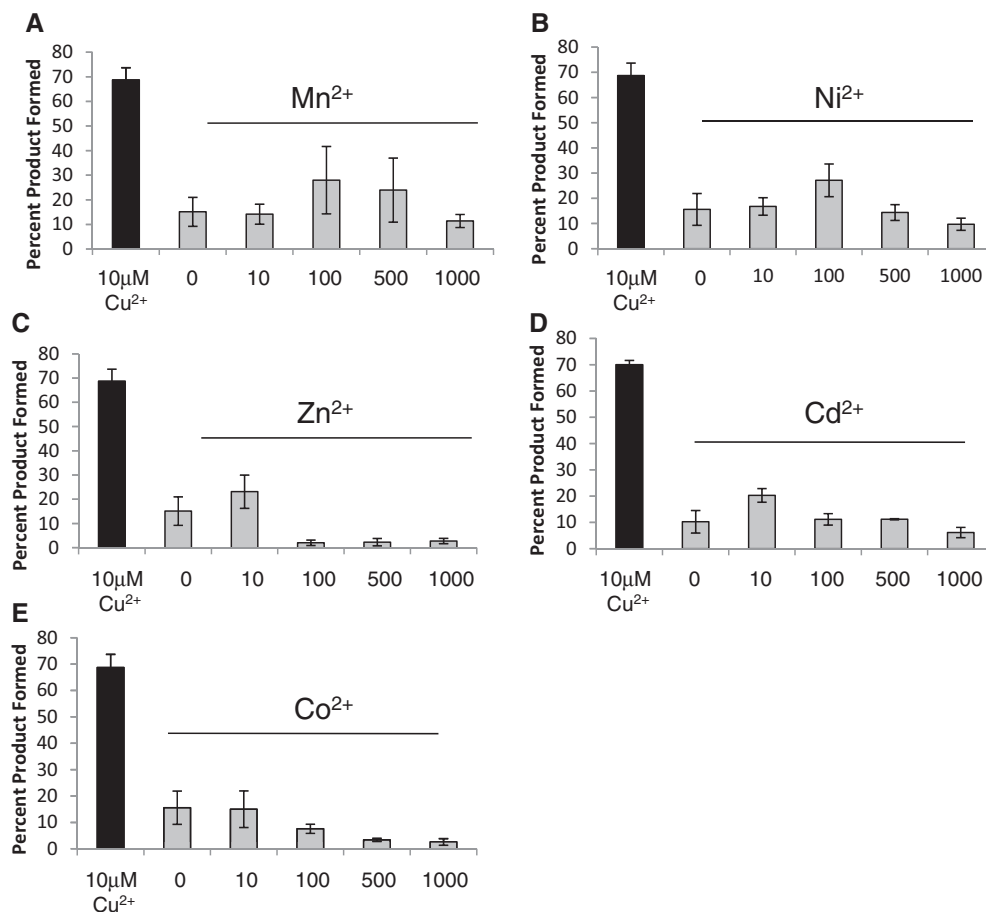
Figure 2. Substitutions for Cu^{2+} reduce or eliminate activity. Product yields were plotted for 18 h self-kinase reactions that were carried out in SP buffers that were modified by replacing 10 μM $CuCl_2$ with $MnCl_2$, $NiCl_2$, $ZnCl_2$, $CdCl_2$ or $CoCl_2$ at the indicated concentrations (grey bars). Yield from a parallel reaction carried out in normal SP buffer ('10 μM Cu^{2+}') is plotted for comparison (black). Average values for four sets of reaction (except for Cd^{2+}, for which N = 2) are plotted. Error bars represent the standard error of the mean.

ILP gives information on conformationally mobile phosphoester bonds that increase the fraction of time in which the 2′OH samples conformations appropriate for in-line attack on the adjacent phosphate and release of the downstream 5′OH (59). No new ILP cleavage was observed when Cu^{2+} was added to the reaction buffer at a concentration of either 10 or 30 μM (Figure 4A, lanes 1–3). In contrast, addition of 0.5 mM GTP induced a strong cleavage after A32, and this cleavage was further sensitized by addition of Cu^{2+} (Figure 4A lanes 4–6). No changes are seen at other positions in response to addition of Cu^{2+} or GTP. These data support direct binding of GTP in the absence of Cu^{2+} and enhanced binding of GTP when Cu^{2+} is present, but they do not provide evidence of a direct interaction between RNA and Cu^{2+} in the absence of GTP. Instead, we interpret the stimulation as indicating that Cu^{2+} binds the triphosphate of GTP in solution, and that the metal-bound form of the GTP makes additional RNA-Cu^{2+} contacts.

Cu^{2+} interacts with the triphosphate region of the phosphoryl donor

Previous studies measured competition for access to the ribozyme active site between GTPγS and a series of substrate analogs (52). GTP, 3′dGTP and a few other analogues were recognized by the RNA and occupied the active site in a manner that prevented GTPγS use. ATP exhibited no such competition and is therefore not believed to interact with the ribozyme. Consistent with this interpretation, the intensity of ILP cleavage at A32 in the presence of 2 mM ATP and 0.5 mM GTP was identical to those observed in reactions without ATP, and addition of excess Cu^{2+} had no effect on the cleavage intensity (Figure 4A, lanes 7 and 8). However, we reasoned that a different mode of competition could result from sequestration of free Cu^{2+} by the triphosphates of other nucleotides, thereby reducing both GTP-induced ILP cleavage and self-thiophosphorylation yield from the GTPγS donor. Furthermore, although Cu^{2+} dependence does not require the sulphur moiety of GTPγS (Figure 2), the presence of the sulphur can be safely assumed to increase affinity of the NTP for Cu^{2+}. Indeed, when ILP was carried out in the presence of 2 mM ATPγS, the cleavage signal at A32 owing to GTP was diminished. Signal strength was partially restored on supplementation with additional Cu^{2+} (Figure 4A, lanes 9 and 10). Quantification of signal strength at position A32 shows that ATPγS reduced total cleavage by ~4.6-fold
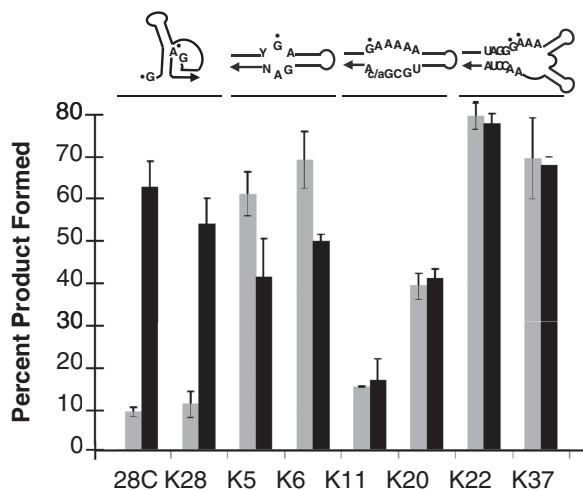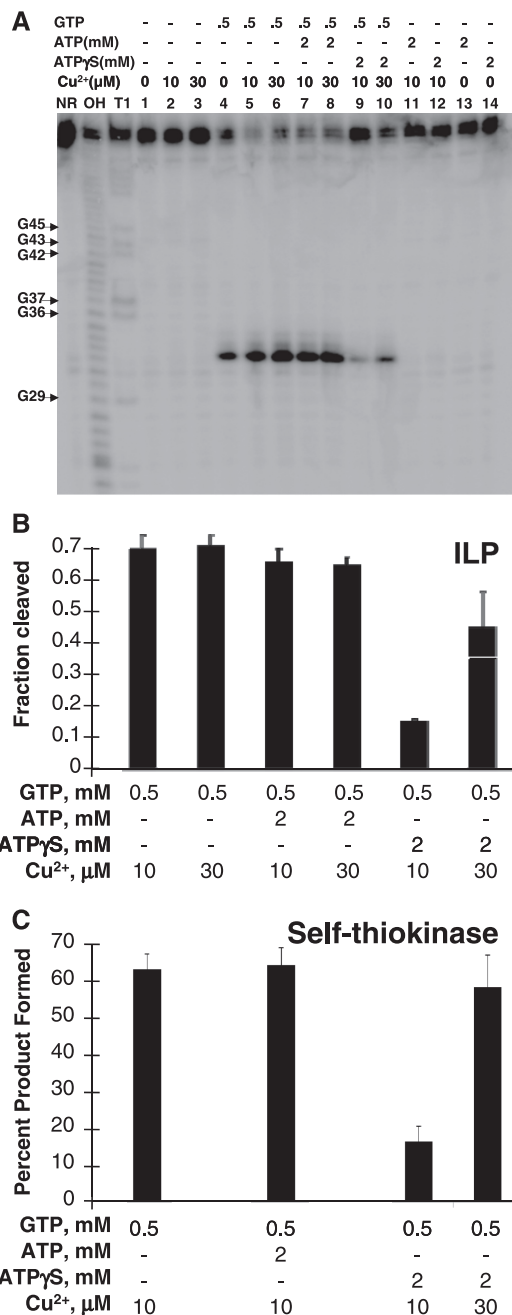
Figure 3. Stimulation by Cu^{2+} is unique to ribozyme K28. Percentage of the indicated ribozymes that were converted to self-thiophosphorylated product is shown for 18-h reaction that was performed in the presence (black) or absence (grey) of $10\,\mu M$ Cu^{2+}. The secondary structural features shared between each pair of ribozymes are indicated above the graph [detailed in ref. (52)]. Asterisks indicate sites of self-thiophosphorylation; '28C' indicates ribozyme K28(1-77)C.

Figure 4. Triphosphate interactions revealed by ILP. ILP analysis was used to determine Cu^{2+}-induced structural changes. (**A**) ILP reactions were performed for 10 h in SP buffer modified to contain 25 mM TRIS (pH 8.0). ATP or ATPγS was added before GTP when both nucleotides were present. For lanes 3, 6, 8 and 10, Cu^{2+} concentration was initially $10\,\mu M$ and was adjusted to $30\,\mu M$ after addition of ATP/ATPγS and GTP. (**B**) Integrated ILP cleavage signal at position A32 under the indicated conditions. (**C**) Chelation-mediated competition in self-thiophosphorylation reactions was evaluated by quantifying product formed after 18 h reactions under the indicated conditions. As aforementioned, competitors were added before addition of GTP, and supplemented Cu^{2+} was added after the addition of competitors and donor.

(Figure 4B). When GTP was omitted from the ILP reaction, neither ATP nor ATPγS induced RNA cleavage at A32, irrespective of Cu^{2+} concentration (Figure 4A, lanes 11–14). These results rule out the possibility of direct RNA–ATP or RNA–ATPγS interactions and suggest that competition by ATPγS is indirect, as would be expected from sequestration of free Cu^{2+} by ATPγS. In the previous analogue studies, GMP competed only weakly with GTPγS, indicating that the beta and gamma phosphates are important for efficient recognition. ILP reactions using GMP in place of GTP gave a Cu^{2+}-dependent cleavage signal at A32 that was much weaker than the GTP-dependent signal, along with faint bands at C39, A46 and C47, all of which were suppressed by ATPγS (Supplementary Figure S1).

The effect of ATPγS on the ribozyme's ability to interact with GTPγS was also examined by monitoring self-thiophosphorylation. Ribozyme K28(1-77)C was incubated overnight with 0.5 mM GTPγS and 2.0 mM ATP or ATPγS. As observed previously (52), excess ATP did not compete and had no effect on reaction yield (Figure 4C). In contrast, ATPγS reduced the observed self-thiophophorylated product by ~3.8-fold, and the addition of supplemental Cu^{2+} restored the yield of thiophosphorylated product. These data establish that Cu^{2+} does interact with the triphosphate region of the nucleotide donor, and that the effects of ATPγS on ILP cleavage and thiophosphoryl transfer is due to chelation of Cu^{2+} by the thiophosphate of ATPγS.
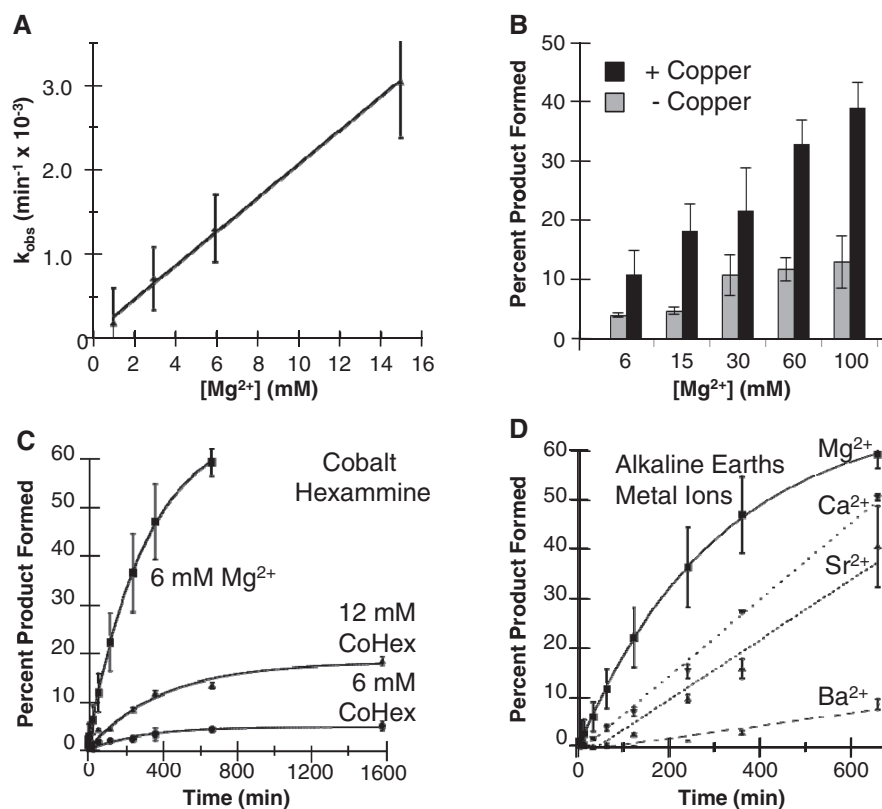
Non-specific Mg^{2+} interactions

Apart from Cu^{2+}, the major divalent ion present during the initial selection was Mg^{2+}. Therefore, all divalent ions except for Cu^{2+} were omitted from SP buffer, and self-thiophosphorylation was monitored for ribozyme K28(1-77)C, as Mg^{2+} concentration was titrated from 0.01 to 15 mM. Thiophosphoryl transfer rates increased linearly from 1 to 15 mM Mg^{2+}, with no indication of approaching saturation over this range (Figure 5A).

Figure 5. Outer-sphere and inner-sphere Mg^{2+} interactions for ribozyme K28(1-77)C. (**A**) Reactions were carried out in the presence of various Mg^{2+} concentrations (0, 0.01, 0.05, 0.1, 0.2, 0.5, 1, 3, 6, and 15 mM). Observed kinetic constants (k_{obs}) are plotted versus Mg^{2+} concentration for reactions in which product was detected. Reactions in which Mg^{2+} was <1 mM yielded insufficient product for accurate determination of k_{obs} and were not plotted. (**B**) Accumulation of thiophosphorylated product in the presence of the indicated Mg^{2+} concentrations after short (3 h) reactions in the presence (black) or absence (grey) of 10 μM Cu^{2+}. (**C**) To evaluate potential inner-sphere Mg^{2+} interactions, kinetic traces were plotted for reactions in which the 6 mM Mg^{2+} component of SP buffer was replaced with 6 or 12 mM CoHex. Uncertainty reported for the rate constants reflects the uncertainties of the fit. (**D**) Similar to part C, except that Mg^{2+} was replaced with other alkaline earth metal ions. Dashed lines indicate linear fits to these data.

Titration with Mn^{2+} yielded a similar pattern as the Mg^{2+} titration to ∼6 mM but was inhibitory at still higher concentrations (data not shown). Little or no product was observed with <1 mM Mg^{2+} or Mn^{2+}, and no product was detected when 6 mM Co^{2+} or Ni^{2+} was used in place of 6 mM Mg^{2+} (data not shown). Thus, Mg^{2+} or Mn^{2+} (or potentially other divalent ions) is required for phosphoryl transfer by K28(1-77)C via low-affinity interactions, but neither divalent cation is specifically required.

Natural kinase and polymerase enzymes make extensive use of Mg^{2+}•NTP and Mg^{2+}•dNTP complexes [see (60–62) and references therein]. However, Cu^{2+} has a higher affinity for phosphates than do Mg^{2+} and other divalent metal ions [>30-fold higher for NMP-metal ion complexes (5)]. Formation of Cu^{2+}•GTPγS is therefore expected to be strongly favoured over formation of Mg^{2+}•GTPγS when both ions are present. To test whether Cu^{2+} dependency at relatively low Mg^{2+} concentrations could be overcome at higher Mg^{2+} concentrations, self-thiophosphorylation yield for relatively short reaction times (3 h) was monitored at Mg^{2+} as high as 100 mM in both the presence and absence of 10 μM Cu^{2+}. As aforementioned, product yield in the presence of Cu^{2+} continued to increase with Mg^{2+} concentration with no sign of approaching saturation (Figure 5B,

black bars). Interestingly, product yield also increased to well above background in the absence of Cu^{2+} at elevated Mg^{2+}, although the yield reached a plateau at ∼30 mM Mg^{2+} and did not approach the yield observed in the presence of Cu^{2+} (Figure 5B, grey bars). Thus, although Mg^{2+} may partially substitute for Cu^{2+} at high concentrations (for example, by forming a Mg^{2+}•GTPγS complex), this partial rescue is only observed when Mg^{2+} is least 3000 times higher than the Cu^{2+} concentration and >15 times higher than the normal Mg^{2+} concentration in SP buffer. It would therefore be premature to infer that the precise contribution of Mg^{2+} at high concentrations is fully interchangeable with the role of 10 μM Cu^{2+}. Overall, the observations from Mg^{2+} titrations suggest that low-affinity, non-specifically bound Mg^{2+} ions serve primarily to aid folding the ribozyme into its active structure, which can then use the Cu^{2+}•GTPγS complex for optimal catalysis.

Evidence for inner sphere interactions with Mg^{2+}

Mg^{2+} can contribute to ribozyme activity by contacting ribozymes and substrates directly (inner sphere), and via ligands such as water that are bound directly to the metal ion (outer sphere). Cobalt hexammine $\{[Co(NH_3)_6]^{3+}$, CoHex} is a reasonably good analogue for outer sphere

interactions with hydrated Mg^{2+} owing to its similar size, geometry and charge, but kinetic stability of the coordinated NH_3 ligands precludes significant inner-sphere interactions. CoHex supports catalysis as well as, or nearly as well as, Mg^{2+} for ribozymes that do not require direct contact with the metal ion, such as the HP ribozyme (26,27,63) and the *in vitro* selected ATRib/AT02 acyltransferase ribozymes (64,65). In contrast, CoHex does not support catalysis at all, or not nearly as well as Mg^{2+}, for ribozymes that exploit direct contacts with the metal ion, such as the HH (44,66), VS (67), RNaseP (68), HDV (69,70) ribozymes and the *in vitro* selected 2PT3.2 kinase ribozyme (51), and CoHex even induces aberrant folding of RNaseP (15).

When the 6 mM Mg^{2+} component of SP was replaced with 6 mM CoHex, self-thiophosphoryl transfer was greatly reduced ($\sim$5% yield after 16 h) (Figure 5C) relative to Mg^{2+} at the same concentration, supporting a potential role for at least one inner-sphere contact with Mg^{2+}. Doubling the CoHex concentration increased yield after 16 h (18%), but the calculated k_{obs} values at these two CoHex concentrations are similar (0.0034 ± 0.0006 and $0.0026 \pm 0.0003 \, min^{-1}$, respectively). Increasing CoHex therefore stimulates the amount of RNA that can self-thiophosphorylate without altering the intrinsic rate. Importantly, the k_{obs} values measured in CoHex/Cu^{2+} are not significantly different from those measured in Mg^{2+}/Cu^{2+} ($0.0032 \pm 0.0001 \, min^{-1}$), even though much more product is formed in Mg^{2+}/Cu^{2+}. Thus, Mg^{2+} plays a role in forming the active structure of ribozyme K28(1-77)C but does not play a catalytic role in thiophosphoryl transfer, even for the Mg^{2+} ions that appear to make inner sphere contacts.

Probing the dimensions of the Mg^{2+}-binding site(s)

To determine whether divalent alkaline earth ions larger than Mg^{2+} could also support catalysis, thiophosphoryl transfer was monitored for reactions in which Ca^{2+}, Sr^{2+} or Ba^{2+} was the only divalent ion apart from 10 μM Cu^{2+}. Replacing 6 mM Mg^{2+} with 6 mM Ca^{2+} or Sr^{2+} produced a modest reduction in overall rate and yield during the 11-h reaction, and much less product formed in 6 mM Ba^{2+} as the major divalent cation (Figure 5D). Interestingly, the rate of product accumulation for these ions is approximately linear rather than fitting well to a first-order kinetic best-fit curve, potentially indicating a shift in the rate-limiting step (e.g. slow folding). These three trends (reductions in rate and yield, and deviation from simple first-order kinetics) all correlate with the ionic radius of these alkaline earth metal ions. Specifically, thiophosphoryl transfer activity decreased in the order $Mg^{2+} > Ca^{2+} > Sr^{2+} \gg Ba^{2+}$, for which the ionic radii of their hexacoordinate forms are 0.86 Å, 1.14 Å, 1.32 Å and 1.49 Å, respectively (71).

pH-dependence

To determine the potential role of proton transfer in the reactivity of ribozyme K28(1-77)C, apparent rate constants were measured, as pH was varied from pH 5.5 to 9.5. Three different buffers were used to span this range

(MES, HEPES and TRIS), including separate reactions in MES or HEPES (pH 6.8) and in HEPES or TRIS (pH 8.0) at the two overlapping pH values to control for buffer-specific effects. In contrast to previously analysed kinase ribozymes (50,51) and DNAzymes (25), for which the rates showed no pH dependence, thiophosphoryl transfer by K28(1-77)C was strongly dependent on pH (Figure 6). The observed first-order rate constants (k_{obs}) increased $\sim$1000-fold from pH 5.5 to 8.5, indicating one proton-transfer event in the rate-limiting step. Fitting these data to a single-proton equation (see 'Materials and Methods' section) yielded an apparent pKa value of 7.99 ± 0.08, and a maximal rate constant ($0.049 \pm 0.002 \, min^{-1}$) that is >15-fold higher than that observed in normal SP buffer. The rate constants for reactions carried out in HEPES were 3–5-fold lower than those for reactions carried out in either MES or TRIS at the two overlapping pH values, and the overall increase with pH was less steep in the presence of HEPES relative to MES or TRIS, indicating buffer-specific effects that make HEPES a suboptimal buffer for ribozyme K28(1-77)C.

DISCUSSION

We demonstrate here that phosphoryl transfer by the K28(1-77)C kinase ribozyme strongly depends on the presence of Cu^{2+}, that the reaction also requires Mg^{2+} or similar divalent cations and that the rate-limiting step of the reaction includes a proton transfer event. Very little product was formed in the absence of Cu^{2+}, independent of whether the donor was GTPγS or [γ-^{32}P]GTP, establishing that the Cu^{2+} requirement persists apart from any potential interaction with the donor sulphur. Fitting the titration data to a binding isotherm indicated a 1:1 stoichiometry, with Kd^{Cu2+} of 0.9 ± 0.4 μM. However, ILP analysis argues against interpreting these data in terms of a simple direct metal ion-RNA interaction, as there
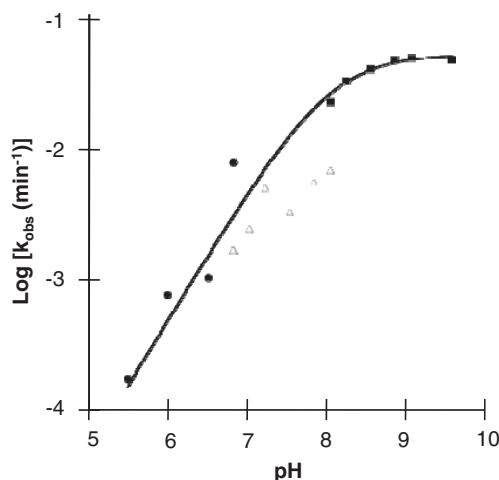
Figure 6. pH rate profile of K28(1-77)C. k_{obs} values are plotted as a function of pH. Because HEPES (triangles) exhibited sub-optimal, buffer-specific effects, only the data from reaction carried out in MES (circles) and TRIS (squares) were used in determining the fit.
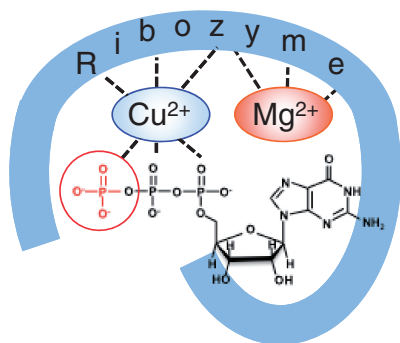
Figure 7. Schematic representation of metal ion interactions in ribozyme K28(1-77)C. Cu^{2+} (blue) is proposed to serve as Lewis acid catalyst by chelating both the nucleotide triphosphate and nucleobase nitrogens within an azophilic binding pocket in the RNA, while Mg^{2+} (red-orange) contributes to structure through both inner sphere and outer sphere interactions. Postulated RNA-GTP interactions through the guanine Watson-Crick face, 3′OH and phosphates are based on previous analysis using analog competition (52).

are no new RNA cleavages associated with addition of Cu^{2+} alone. Instead Cu^{2+} stimulates GTP-dependent RNA cleavage and partially alleviates the inhibitory effects of competitor ATPγS on RNA cleavage during ILP and on product formation during self-thiophosphorylation reactions. All of these observations suggest that Cu^{2+} enters the ribozyme as a Cu^{2+}•GTPγS chelation complex, wherein it is additionally chelated by a nitrogen-rich site in the RNA (Figure 7). Cu^{2+} is highly azaphilic and prone to Jahn-Teller geometry distortions in certain binding environments. As such, it may be particularly well suited to bind within a nitrogenous pocket that is unable to form strong interactions with other metal ions. Such interactions would ideally position the metal ion to promote the chemical step of the reaction by withdrawing electrons from the phosphate (Lewis acid catalysis), making it more susceptible to nucleophilic attack by the acceptor oxygen. In addition, Cu^{2+} binds phosphate more tightly than do the other metal ions assayed here (5,58), and phosphodiester cleavage rates by HH ribozymes in various metal ions correlate with binding affinities of those metal ions with phosphate monoesters (5). However, phosphate affinity alone does not explain metal ion selectivity, as these other metals cannot fully substitute for Cu^{2+} even at 100-fold (for transition metal ions) to >1000-fold (for Mg^{2+}) higher concentrations. Partial rescue in the absence of Cu^{2+} at very high Mg^{2+} concentrations suggests that the Mg^{2+}•GTPγS complex can also be used. However, the yield of thiophosphorylated product in the presence of Cu^{2+} continues to increase well above the Mg^{2+} concentration where the yield saturates in the absence of Cu^{2+}, indicating that the Mg^{2+}•GTPγS is not used by the ribozyme as well as the Cu^{2+}•GTPγS complex. We therefore propose that Cu^{2+} ion selectivity results from a combination of coordination geometry, azaphilicity, geometric constraints of the active site and affinity for phosphates.

Apart from K28(1-77)C, there are few or no other Cu^{2+}-dependent ribozymes available for comparison. A Diels–Alderase ribozyme selected in the presence of Mn^{2+}, Fe^{2+},

Co^{2+}, Ni^{2+}, Cu^{2+}, Cd^{2+} and Zn^{2+} was initially reported as requiring Cu^{2+} (72,73). They interpreted the Cu^{2+} requirement in terms of catalytic Cu^{2+} Lewis acid sites, consistent with Lewis acid-catalysed Diels–Alder reactions in water. However, one of those Diels–Alderase ribozymes was later shown to function in the absence of Cu^{2+}, given elevated concentrations of Mg^{2+}, thereby establishing that Cu^{2+} plays a non-essential role in that ribozyme (74). Nevertheless, Lewis acid catalysis figures prominently in ribozyme reactions related to phosphoryl transfer. For example, a recent crystal structure of the HDV ribozyme shows inner-sphere ligand interactions between an active site Mg^{2+} ion and the pro-R(P) oxygen of the scissile phosphate and the 2′-hydroxyl nucleophile (75). Similarly, polymerase and pyrophosphatase enzymes (which formally catalyse phosphoryl transfer to a polynucleotide chain or to water) use two Mg^{2+} ions as Lewis acid catalysts to shield charges and lower the pKa of the leaving group (62).

The reduction in overall thiophosphoryl transfer activity by ribozyme K28(1-77)C on replacing Mg^{2+} with the non-exchanging CoHex indicates that the ribozyme takes advantage of inner sphere interactions with Mg^{2+}; however, the primary role of Mg^{2+} is to help establish the active structure, as evidenced by the insensitivity of the first-order rate constants to the CoHex substitution. Larger alkaline earth metal ions also promoted self-thiophosphorylation, but they did so less well and induced an intriguing and increasingly prominent deviation from first-order kinetic behaviour. The correlation of these trends with ionic radius may reflect simple steric constraints (upper size limit on ions that can successfully replace Mg^{2+} in at least one specific binding site), or they may arise from chemical features of the ions that also correlate with ionic radius, such as increased polarizability or reduced charge density.

In addition to its unusual metal ion requirements, K28(1-77)C is also the first kinase ribozyme to demonstrate a dependence on pH. Prior work with ribozymes Kin.46 (50) and 2PT3.2 min (51) observed no change in reaction rates, as pH were varied over several pH units. These observations suggested that deprotonation and activation of the 2′OH acceptor nucleophile was not rate limiting for those ribozymes and potentially suggested an S_N1-like dissociative mechanism in which release of the gamma (thio)phosphate from the donor precedes formation of the acceptor-phosphate bond (50). The log-linear increase in the pH rate profiles observed here indicates that deprotonation of a species with pKa of 7.99 $\pm$ 0.08 is required for maximal thiophosphoryl transfer activity. The ribose 2′OH at the two modification sites are logical candidates for deprotonation to increase their nucleophilicity for attack on the gamma phosphate. However, the pKa for a ribose 2′OH is in the range of 12.2–13.7 (52,76,77) and would need to be perturbed four to five pH units to account for the data here. The pKa for hydrated Mg^{2+} (11.4) is closer to the observed kinetic pKa, but the essentially unperturbed k_{obs} in CoHex argues against a catalytic role for Mg^{2+}. The pKa values for free guanosine (N1)H and uridine (N3)H are each $\sim$9.2 and could be shifted to near 8.0 within the context

of the ribozyme active site, for example, via metal ion interactions (9,44). Intriguingly, the pKa of Cu^{2+}-bound water is near 7.5 (71,78) and is expected to shift upward in complexes with ligands that donate electrons to the metal ion centre. Deprotonation of one of the waters on a bound (inner sphere, partially dehydrated) catalytic copper hydrate or Cu^{2+}-nucleobase interactions that modulate the pKa of the nucleobase would provide an intriguing functional linkage between the Cu^{2+} requirement and pH sensitivity of this kinase ribozyme.

Although HEPES is generally considered to be a non-chelating buffer with respect to hard metal ions such as Mg^{2+} (79), interactions between Cu^{2+} and HEPES have been observed by isothermal titration calorimetry (80), electron paramagnetic resonance spectroscopy (81) and potentiometric titrations (81,82). However, the suboptimal performance of HEPES buffer is not fully explained by a simple competition between the buffer and the ribozyme/donor for access to the metal ion; TRIS buffer forms TRIS•Cu^{2+} chelates with affinities that are similar to those of the HEPES•Cu^{2+} complex (58,81) and yet is well behaved with respect to its influence on the pH dependence of the reaction rate. Buffer-specific effects were not further explored.

In conclusion, the chemical mechanism of the ribozyme K28(1-77)C stands in sharp contrast with previously characterized kinase ribozymes, using a tightly bound Cu^{2+} ion and also using a species that deprotonates with pKa $\approx$ 8.0, in addition to specifically bound (potentially inner sphere) and non-specific cations required for folding. The contributions of Cu^{2+} to the catalytic mechanism include unique chemical features that cannot be provided by other first-row transition metal ions and that appear to implicate Lewis acid catalysis through Cu^{2+} chelation by the incoming donor triphosphate in a Cu^{2+}•GTP or Cu^{2+}•GTPγS complex. The chemical strategies that ribozymes K28 and its derivatives use to accomplish (thio)phosphoryl transfer are clearly distinct from those used by other kinase ribozymes to perform the same reaction, including those that were co-selected along with K28 under identical ionic conditions. An implication for RNA world theories is that the parallel evolution of strikingly diverse metal ion and pH requirements among ribozymes within a single population highlights the ability of RNA to evolve structures that capitalize on a diverse suite of mechanisms and local resources to accomplish the same chemical objectives.

SUPPLEMENTARY DATA

Supplementary Data are available at NAR Online: Supplementary Figure 1.

ACKNOWLEDGEMENTS

FUNDING

REFERENCES

1. Roth,A. and Breaker,R.R. (1998) An amino acid as a cofactor for a catalytic polynucleotide. *Proc. Natl Acad. Sci. USA*, **95**, 6027–6031.
2. Tsukiji,S., Pattnaik,S. and Suga,H. (2003) An alcohol dehydrogenase ribozyme. *Nat. Struct. Biol.*, **10**, 713–717.
3. Tsukiji,S., Pattnaik,S. and Suga,H. (2004) Reduction of an aldehyde by a NADH/Zn^{2+} -dependent redox active ribozyme. *J. Am. Chem. Soc.*, **126**, 5044–5045.
4. Gong,B., Klein,D., Ferré-D'Amaré,A. and Carey,P. (2011) The glmS ribozyme tunes the catalytically critical pK(a) of its coenzyme glucosamine-6-phosphate. *J. Am. Chem. Soc.*, **133**, 14188–14191.
5. Schnabl,J. and Sigel,R. (2010) Controlling ribozyme activity by metal ions. *Curr. Opin. Chem. Biol.*, **14**, 269–275.
6. Irving,H. and Williams,R. (1953) The stability of transition-metal complexes. *J. Chem. Soc.*, 3192–3210.
7. Sigel,H., Hofstetter,F., Martin,R.B., Milburn,R.M., Scheller-Krattiger,V. and Schellerla,K.H. (1984) General considerations on transphosphorylations: mechanism of the metal ion facilitated dephosphorylation of nucleoside 5′-triphosphates, including promotion of atp dephosphorylation by addition of adenosine 5′-monophosphate. *J. Am. Chem. Soc.*, **106**, 7935–7946.
8. Athavale,S., Petrov,A., Hsiao,C., Watkins,D., Prickett,C., Gossett,J., Lie,L., Bowman,J., O'Neill,E., Bernier,C. *et al.* (2012) RNA folding and catalysis mediated by iron (II). *PLoS One*, **7**, e38024.
9. Roychowdhury-Saha,M. and Burke,D. (2006) Extraordinary cleavage rates in transition metal ion mediated catalysis by a tertiary stabilized hammerhead ribozyme. *RNA*, **12**, 1846–1852.
10. Horton,T., Clardy,D. and DeRose,V. (1998) Electron paramagnetic resonance spectroscopic measurement of Mn^{2+} binding affinities to the hammerhead ribozyme and correlation with cleavage activity. *Biochemistry*, **37**, 18094–18101.
11. Hunsicker,L. and DeRose,V. (2000) Activities and relative affinities of divalent metals in unmodified and phosphorothioate-substituted hammerhead ribozymes. *J. Inorg. Biochem.*, **80**, 271–281.
12. Long,D., LaRiviere,F. and Uhlenbeck,O. (1995) Divalent metal ions and the internal equilibrium of the hammhead ribozyme. *Biochemistry*, **34**, 14435–14440.
13. Peracchi,A., Beigelman,L., Scott,E., Uhlenbeck,O. and Herschlag,D. (1997) Involvement of a specific metal ion in the transition of the hammerhead ribozyme to its catalytic conformation. *J. Biol. Chem.*, **272**, 26822–26826.
14. Markley,J.C., Godde,F. and Sigurdsson,S.T. (2001) Identification and characterization of a divalent metal ion-dependent cleavage site in the hammerhead ribozyme. *Biochemistry*, **40**, 13849–13856.
15. Cuzic,S. and Hartmann,R. (2005) Studies on Escherichia coli RNase P RNA with Zn^{2+} as the catalytic cofactor. *Nucleic Acids Res.*, **33**, 2464–2474.
16. Hati,S., Boles,A.R., Zaborske,J.M., Bergman,B., Posto,A.L. and Burke,D.H. (2003) $Nickel^{2+}$-mediated assembly of an RNA-amino acid complex. *Chem. Biol.*, **10**, 1129–1137.
17. Ciesiolka,J., Gorski,J. and Yarus,M. (1995) Selection of an RNA domain that binds Zn^{2+}. *RNA*, **1**, 538–550.
18. Li,Y. and Sen,D. (1998) The modus operandi of a DNA enzyme: enhancement of substrate basicity. *Chem. Biol.*, **5**, 1–12.

19. Li,Y. and Sen,D. (1996) A catalytic DNA for porphyrin metallation. *Nat. Struct. Biol.*, **3**, 743–747.
20. Cuenoud,B. and Szostak,J.W. (1995) A DNA metalloenzyme with DNA ligase activity. *Nature*, **375**, 611–614.
21. Carmi,N., Balkhi,S. and Breaker,R. (1998) Cleaving DNA with DNA. *Proc. Natl Acad. Sci. USA*, **95**, 2233–2237.
22. Carmi,N. and Breaker,R.R. (2001) Characterization of a DNA-cleaving deoxyribozyme. *Bioorg. Med. Chem.*, **9**, 2589–2600.
23. Li,Y., Liu,Y. and Breaker,R. (2000) Capping DNA with DNA. *Biochemistry*, **39**, 3106–3114.
24. McManus,S. and Li,Y. (2008) A deoxyribozyme with a novel guanine quartet pseudoknot structures. *J. Mol. Biol.*, **375**, 960–968.
25. Wang,W., Billen,L.P. and Li,Y. (2002) Sequence diversity, metal specificity, and catalytic proficiency of metal-dependent phosphorylating DNA enzymes. *Chem. Biol.*, **9**, 507–517.
26. Hampel,A. and Cowan,J. (1997) A unique mechanism for RNA catalysis: the role of metal cofactors in hairpin ribozyme cleavage. *Chem. Biol.*, **4**, 513–517.
27. Nesbitt,S., Hegg,L. and Fedor,M. (1997) An unusual pH-independent and metal-ion-independent mechanism for hairpin ribozyme catalysis. *Chem. Biol.*, **4**, 619–630.
28. Young,K., Gill,F. and Grasby,J. (1997) Metal ions play a passive role in the hairpin ribozyme catalysed reaction. *Nucleic Acids Res.*, **25**, 3760–3766.
29. Murray,J., Seyhan,A., Walter,N., Burke,J. and Scott,W. (1998) The hammerhead, hairpin and VS ribozymes are catalytically proficient in monovalent cations alone. *Chem. Biol.*, **5**, 587–595.
30. Curtis,E. and Bartel,D. (2001) The hammerhead cleavage reaction in monovalent cations. *RNA*, **7**, 546–552.
31. Bevilacqua,P., Brown,T., Nakano,S. and Yajima,R. (2004) Catalytic roles for proton transfer and protonation in ribozymes. *Biopolymers*, **73**, 90–109.
32. Nakano,S., Chadalavada,D. and Bevilacqua,P. (2000) General acid-base catalysis in the mechanism of a hepatitis delta virus ribozyme. *Science*, **287**, 1493–1497.
33. Shih,I. and Been,M. (2001) Involvement of a cytosine side chain in proton transfer in the rate-determining step of ribozyme self-cleavage. *Proc. Natl Acad. Sci.*, **98**, 1489–1494.
34. Ferré-D'Amaré,A., Zhou,K. and Doudna,J. (1998) Crystal structure of a hepatitis delta virus ribozyme. *Nature*, **395**, 567–574.
35. Han,J. and Burke,J. (2005) Model for general acid-base catalysis by the hammerhead ribozyme: pH-activity relationships of G8 and G12 variants at the putative active site. *Biochemistry*, **44**, 7864–7870.
36. Martick,M. and Scott,W. (2006) Tertiary contacts distant from the active site prime a ribozyme for catalysis. *Cell*, **126**, 309–320.
37. Smith,M., Mehdizadeh,R., Olive,J. and Collins,R. (2008) The ionic environment determines ribozyme cleavage rate by modulation of nucleobase pKa. *RNA*, **14**, 1942–1949.
38. Kuzmin,Y., Da Costa,C., Cottrell,J. and Fedor,M. (2005) Role of an active site adenine in hairpin ribozyme catalysis. *J. Mol. Biol.*, **349**, 989–1010.
39. Cottrell,J., Scott,L. and Fedor,M. (2011) The pH dependence of hairpin ribozyme catalysis reflects ionization of an active site adenine. *J. Biol. Chem.*, **286**, 17658–17664.
40. Ditzler,M., Sponer,J., and NG,W. (2009). NGW. (2009) Molecular dynamics suggest multifunctionality of an adenine imino group in acid-base catalysis of the hairpin ribozyme. *RNA*, **15**, 560–575.
41. Chi,Y., Martick,M., Lares,M., Kim,R., Scott,W. and Kim,S. (2008) Capturing hammerhead ribozyme structures in action by modulating general base catalysis. *PLoS Biol.*, **6**, e234.
42. Lambert,D., Heckman,J. and Burke,J. (2006) Three conserved guanosines approach the reaction site in native and minimal hammerhead ribozymes. *Biochemistry*, **45**, 140–147.
43. Thomas,J. and Perrin,D. (2008) Probing general base catalysis in the hammerhead ribozyme. *J. Am. Chem. Soc.*, **130**, 15467–15475.
44. Roychowdhury-Saha,M. and Burke,D. (2007) Distinct reaction pathway promoted by non-divalent-metal cations in a tertiary stabilized hammerhead ribozyme. *RNA*, **13**, 841–848.
45. Martick,M., Lee,T., York,D. and Scott,W. (2008) Solvent structure and hammerhead ribozyme catalysis. *Chem. Biol.*, **15**, 332–342.
46. Klein,D., Been,M. and Ferré-D'Amaré,A. (2007) Essential role of an active-site guanine in glmS ribozyme catalysis. *J. Am. Chem. Soc.*, **129**, 14858–14859.
47. Cochrane,J., Lipchock,S., Smith,K. and Strobel,S. (2009) Structural and chemical basis for glucosamine 6-phosphate binding and activation of the glmS ribozyme. *Biochemisry*, **48**, 3239–3246.
48. Wedekind,J. (2011) Metal ion binding and function in natural and artificial small RNA enzymes from a structural perspective. *Met. Ions Life Sci.*, **9**, 299–345.
49. Viladoms,J., Scott,L. and Fedor,M. (2011) An active-site guanine participates in glmS ribozyme catalysis in its protonated state. *J. Am. Chem. Soc.*, **133**, 18388–18396.
50. Lorsch,J.R. and Szostak,J.W. (1995) Kinetic and thermodynamic characterization of the reaction catalyzed by a polynucleotide kinase ribozyme. *Biochemistry*, **34**, 15315–15327.
51. Saran,D., Nickens,D. and Burke,D. (2005) A trans acting ribozyme that phosphorylates exogenous RNA. *Biochemistry*, **44**, 15007–15016.
52. Biondi,E., Nickens,D.G., Warren,S., Saran,D. and Burke,D.H. (2010) Convergent donor and acceptor substrate utilization among kinase ribozymes. *Nucleic Acids Res.*, **38**, 6785–6795.
53. Biondi,E., Maxwell,A. and Burke,D. (2012) A small kinase ribozyme with dual-site activity. *Nucleic Acids Res.*, **40**, 7528–7540.
54. Igloi,G.L. and Kossel,H. (1985) Affinity electrophoresis for monitoring terminal phosphorylation and the presence of queuosine in RNA. Application of polyacrylamide containing a covalently bound boronic acid. *Nucleic Acids Res.*, **13**, 6881–6898.
55. Igloi,G. (1988) Interaction of tRNAs and of phosphorothioate-substituted nucleic acids with an organomercurial. Probing the chemical environment of thiolated residues by affinity electrophoresis. *Biochemistry*, **27**, 3842–3849.
56. Rhee,S. and Burke,D. (2004) Tris(2-carboxyethyl)phosphine stabilization of RNA: comparison with dithiothreitol for use with nucleic acid and thiophosphoryl chemistry. *Anal. Biochem.*, **325**, 137–143.
57. Pearson,R. (1963) Hard and Soft Acids and Bases. *J. Am. Chem. Soc.*, **85**, 3533–3539.
58. Sigel,H. and Griesser,R. (2005) Nucleoside 5′-triphosphates: self-association, acid–base, and metal ion- binding properties in solution. *Chem. Soc. Rev.*, **34**, 875–900.
59. Soukup,G. and Breaker,R. (1999) Relationship between internucleotide linkage geometry and the stability of RNA. *RNA*, **5**, 1308–1325.
60. Adams,J. (2001) Kinetic and catalytic mechanisms of protein kinases. *Chem. Rev.*, **101**, 2271–2290.
61. Batra,V., Beard,W., Shock,D., Krahn,J., Pedersen,L. and Wilson,S. (2006) Magnesium-induced assembly of a complete DNA polymerase catalytic complex. *Structure*, **14**, 757–766.
62. Steitz,T. and Steitz,J. (1993) A general two-metal-ion mechanism for catalytic RNA. *Proc. Natl Acad. Sci. USA.*, **90**, 6498–6502.
63. Walter,F., Murchie,A., Thomson,J. and Lilley,D. (1998) Structure and activity of the hairpin ribozyme in its natural junction conformation: effect of metal ions. *Biochemistry*, **37**, 14195–14203.
64. Suga,H., Cowan,J.A. and Szostak,J.W. (1998) Unusual metal ion catalysis in an acyl-transferase ribozyme. *Biochemistry*, **37**, 10118–10125.
65. Lee,N. and Suga,H. (2001) Essential roles of innersphere metal ions for the formation of the glutamine binding site in a bifunctional ribozyme. *Biochemistry*, **40**, 13633–13643.
66. Horton,T. and DeRose,V. (2000) Cobalt hexammine inhibition of the hammerhead ribozyme. *Biochemisry*, **39**, 11408–11416.
67. Maguire,J. and Collins,R. (2001) Effects of cobalt hexammine on folding and self-cleavage of the Neurospora VS ribozyme. *J. Mol. Biol.*, **309**, 45–56.
68. Kurz,J. and Fierke,C. (2002) The affinity of magnesium binding sites in the Bacillus subtilis RNase P x pre-tRNA complex is enhanced by the protein subunit. *Biochemistry*, **41**, 9545–9558.

69. Ke,A., Ding,F., Batchelor,J. and Doudna,J. (2007) Structural roles of monovalent cations in the HDV ribozyme. *Structure*, **15**, 281–287.

70. Gong,B., Chen,J., Bevilacqua,P., Golden,B. and Carey,P. (2009) Competition between Co(NH(3)(6)3+ and inner sphere Mg^{2+} ions in the HDV ribozyme. *Biochemistry*, **48**, 11961–11970.

71. Huheey,J. (1983) *Inorganic Chemistry. Principles of Structure and Reactivity*, 3 edn. Harper & Row, New York.

72. Tarasow,T.M., Tarasow,S.L. and Eaton,B.E. (1997) RNA-catalyzed carbon-carbon bond formation. *Nature*, **389**, 54–57.

73. Tarasow,T., Tarasow,S. and Eaton,B. (2000) RNA diels-alderase: relationships between unique seuqences and catalytic functions. *J. Am. Chem. Soc.*, **122**, 1015–1021.

74. Gagnon,K., Ju,S.-Y., Goshe,M., Maxwell,E. and Franzen,S. (2009) A role for hydrophobicity in a Diels–Alder reaction catalyzed by pyridyl-modified RNA. *Nucleic Acids Res.*, **37**, 3074–3082.

75. Chen,J., Yajima,R., Chadalavada,D., Chase,E., Bevilacqua,P. and Golden,B. (2010) A 1.9 A crystal structure of the HDV ribozyme precleavage suggests both Lewis acid and general acid mechanisms contribute to phosphodiester cleavage. *Biochemistry*, **49**, 6508–6518.

76. Velikyan,I., Acharya,S., Trifonova,A., Foldesi,A. and Chattopadhyaya,J. (2001) The pKa's of 2′-hydroxyl groups in nucleosides and nucleotides. *J. Am. Chem. Soc.*, **123**, 2983–2984.

77. Li,Y. and Breaker,R. (1999) Kinetics of specific base catalysis of RNA degradation by transesterification involving the 2′-hydroxyl group. *J. Am. Chem. Soc.*, **121**, 5364–5372.

78. Burgess,J. (1978) *Metal Ions in Solution*. Ellis Horwood Ltd, London.

79. Good,N., Winget,G., Winter,W., Connolly,T., Izawa,S. and Singh,R. (1966) Hydrogen ion buffers for biological research. *Biochemistry*, **5**, 467–474.

80. Quinn,C. (2010) Analyzing ITC data for the enthalpy of binding metal ions to ligands. *TA Instruments Application Note*, **MCAPN-2010-02**, 1–6.

81. Sokołowska,M. and Bal,W. (2005) Cu(II) complexation by "non-coordinating" N-2-hydroxyethylpiperazine-N′-2-ethanesulfonic acid (HEPES buffer). *J. Inorg. Bioch.*, **99**, 1653–1660.

82. Mash,H., Chin,Y., Sigg,L., Hari,R., and H,X. (2003). HX. (2003) Complexation of copper by zwitterionic aminosulfonic (Good) buffers. *Anal. Chem.*, **75**, 671–677.